The FASEB Journal article fj.13-228973. Published online May 2, 2013.

Molecular components required for resting and stimulated endocytosis of botulinum neurotoxins by glutamatergic and peptidergic neurons

Jianghui Meng, Jiafu Wang, Gary W. Lawrence, and J. Oliver Dolly[1]

International Centre for Neurotherapeutics, Dublin City University, Dublin, Ireland

ABSTRACT **Proteins responsible for basal and stimulated endocytosis in nerves containing small clear synaptic vesicles (SCSVs) or large dense-core vesicles (LDCVs) are revealed herein, using probes that exploit surface-exposed vesicle proteins as acceptors for internalization. Basal uptake of botulinum neurotoxins (BoNTs) by both SCSV-releasing cerebellar granule neurons (CGNs) and LDCV-enriched trigeminal ganglionic neurons (TGNs) was found to require protein acceptors and acidic compartments. In addition, dynamin, clathrin, adaptor protein complex-2 (AP2), and amphiphysin contribute to the depolarization-evoked entry. For fast recycling of SCSVs, knockdown and knockout strategies demonstrated that CGNs use predominantly dynamin 1, whereas isoform 2 and, to a smaller extent, isoform 3 support a less rapid mode of stimulated endocytosis. Accordingly, proximity ligation assay confirmed that dynamin 1 and 2 colocalize with amphiphysin 1 in CGNs, and the latter copurified with both dynamins from cell extracts. In contrast, LDCV-releasing TGNs preferentially employ dynamins 2 and 3 and amphiphysin 1 for evoked endocytosis and lack the fast phase. Hence, stimulation recruits dynamin, clathrin, AP2, and amphiphysin to augment BoNT internalization, and neurons match endocytosis mediators to the different demands for locally recycling SCSVs or replenishing distally synthesized LDCVs.—Meng, J., Wang, J., Lawrence, G. W., Dolly, J. O. Molecular components required for resting and stimulated endocytosis of botulinum neurotoxins by glutamatergic and peptidergic neurons. *FASEB J.* 27, 000–000 (2013). www.fasebj.org**

Key Words: amphiphysin · AP2 · clathrin · dynamin · large dense-core vesicles · small clear synaptic vesicles

THERE IS A GREAT need to decipher the uptake processes in different types of neurons for the 7 serotypes of botulinum neurotoxin (BoNT) due to these being the most potent poison known, causing life-threatening botulism by intracellularly inhibiting transmitter release (reviewed in refs. 1, 2). Furthermore, clinical use of innocuous, tiny amounts of the toxin for treating neuronal disorders has kindled interest in the molecular machinery responsible for their trafficking. Type A BoNT (BoNT/A) has proved successful in alleviating the symptoms of >100 conditions arising from nerve overactivity, *e.g.*, dystonias, spasticity, autonomic hypersecretory disorders, and overactive bladder (reviewed in ref. 3). Also, it can reduce the frequency of chronic migraine and chronic daily headaches (4), although not all types of chronic pain are responsive (5).

BoNTs consist of a proteolytic light chain linked *via* a disulfide and noncovalent bonds to a heavy chain (HC). These neurotoxic proteins bind to intravesicular regions of synaptic vesicle protein 2 (SV2; BoNT/A, /D, /E, and /F) or synaptotagmin (BoNT/B and /G) that become exposed on exocytosis and, thereby, enter neurons by exploiting the recycling of small clear synaptic vesicles (SCSVs; refs. 6–15). Hence, BoNT uptake is accelerated by nerve stimulation (16–18). In comparison, little is known regarding the mode of BoNT entry into nerves that mainly secrete neuropeptides from large dense-core vesicles (LDCVs), such as sensory fibers. Study of the toxins' entry into different neuron types is warranted due to the prospect of yielding insights into differences and commonalities

Abbreviations: ADBE, activity-dependent bulk endocytosis; Amph, amphiphysin; AP2, adaptor protein complex 2; Baf A1, bafilomycin A1; BoNT, botulinum neurotoxin; CCP, clathrin-coated pit; CGN, cerebellar granule neuron; HC, heavy chain; HK, high K^+ concentration; Ht, heterozygous; KD, knockdown; KO, knockout; LDCV, large dense-core vesicle; LK, low K^+ concentration; MT, mutant BoNT/B; PLA, proximity ligation assay; SCSV, small clear synaptic vesicle; SNAP-25, synaptosome-associated protein of molecular mass of ~25 kDa; SNARE, soluble *N*-ethylmaleimide-sensitive factor attachment protein receptor; SV2, synaptic vesicle protein 2; SV2C-L4, SV2C luminal domain 4; SypHluorin, synaptophysin-pHluorin; Syt-ecto, monoclonal antibody to an intraluminal epitope of synaptotagmin I; TGN, trigeminal ganglionic neuron; vH^+-ATPase, vacuolar (v-type) H^+-ATPase; VAMP2, vesicle-associated membrane protein isoform 2; WT, wild type

[1] Correspondence: International Centre for Neurotherapeutics, Dublin City University, Glasnevin, Dublin 9, Ireland. E-mail: oliver.dolly@dcu.ie

doi: 10.1096/fj.13-228973

This article includes supplemental data. Please visit *http://www.fasebj.org* to obtain this information.

between the processes employed to recycle SCSVs and replenish LDCVs. For example, SCSVs are mostly regenerated and refilled with transmitters close to their release sites, while LDCV membrane components pass through endosomal compartments and the Golgi complex before reutilization (19). On endocytosis, BoNTs translocate their enzymatic moiety from acidic compartments into the cytosol (20), where they cleave soluble *N*-ethylmaleimide-sensitive factor attachment protein receptors (SNAREs). Removal of 9 and 26 C-terminal residues from synaptosomal-associated protein of molecular mass of ~25 kDa (SNAP-25) by BoNT type A and E, respectively, inactivates its functioning in SNARE-mediated exocytosis; conveniently, this provides a sensitive measure of the toxins' entry. On the other hand, BoNT/B, /D, /F, and /G cleave vesicle-associated membrane protein (VAMP; reviewed in ref. 3).

Recycling of SCSVs requires dynamin, clathrin [plus its adaptor protein complex (AP)], and amphiphysin (Amph; ref. 21). Dynamins are a family of large GTPases (molecular mass ~100 kDa), encoded by 3 genes showing ~79% amino acid sequence identity, which play critical roles in the scission of invaginated vesicles (21). Drug-induced inhibition of the GTPase of dynamins delays neuroparalysis by BoNT/A (22), but, notably, the isoforms involved have not been identified. Clathrin self-assembles its heavy and light chains into triskelion structures to coat endocytotic vesicles. This entails its recruitment to membranes by binding to AP2, which clusters receptors and their ligands into clathrin-coated pits (CCPs; refs. 23–25). Clathrin participates in dynamin-mediated basal uptake of the BoNT/A C-terminal moiety of HC into neuroblastoma-glioma hybrid cells and, to a lesser extent, intestinal cells (26). The question remains as to whether the internalization of full-length BoNT shares these requirements in primary neurons. Amph 1 and 2 are homologous (~49%) proteins that generate membrane curvature and recruit dynamins to the neck of CCPs before the formation of coated invaginations and eventual scission (27, 28). Amphs are enriched at nerve terminals on SCSVs as well as in the cytosol. They form homo- and heterodimers and, like dynamins, are dephosphorylated in response to increases in intracellular [Ca^{2+}] (28).

To gain insights into the distinct cellular and molecular aspects of endocytosis in neurons, especially on the isoforms of dynamin and Amph utilized in the membrane recycling that is exploited by BoNTs, their uptake was investigated using cerebellar granule neurons (CGNs, which mainly release glutamate from SCSVs) and trigeminal ganglionic neurons (TGNs, known to largely store and secrete neuropeptides from LDCVs). The latter are of particular interest, as inhibition of their release has been implicated in the attenuation by BoNT/A of some forms of chronic pain (reviewed in ref. 3). Knockdown (KD) and knockout (KO) strategies were used in combination with selective inhibitors to ascertain the involvement of the aforementioned proteins in basal or K^+-stimulated uptake of BoNT. CGNs and TGNs were found to internalize BoNT/A and a chimera of BoNT/E and /A (EA) *via* a slow process in resting neurons that does not involve dynamin but requires protein acceptors and acidified compartments, and a depolarization-induced, acceptor-dependent predominant mode that depends on vacuolar (v-type) H^+-ATPase (vH^+-ATPase) activity plus dynamin, clathrin, AP2, and Amph. This is the first direct demonstration that BoNTs enter neurons *via* both dynamin/clathrin/AP2-dependent and -independent endocytosis. Moreover, differential utilization of individual dynamins or Amphs was uncovered in the 2 different neuron types, related to their need for distinct trafficking routes. Dynamin 1 supports the fastest phase of synaptophysin-pHluorin (SypHluorin) endocytosis in CGNs but not the slow LDCV retrieval in TGNs, which is mediated by isoforms 2 and 3.

MATERIALS AND METHODS

Ethics statement

The experiments and maintenance and care of the rodents complied with the European Communities (Amendment of Cruelty to Animals Act 1876) Regulations 2002 and 2005. Experimental procedures have been approved by the Research Ethics Committee of Dublin City University and licensed by the Irish authorities (permit 100/3609).

Animals

Dynamin 1 heterozygous (Ht) mice were kindly provided by Pietro De Camilli (Yale University, New Haven, CT, USA) and bred in-house, and littermates were genotyped. Pups from rats (Sprague-Dawley) or mice (a mix of 129SV/J and C57Bl6) and Thy1-YFP transgenic mice (The Jackson Laboratory, Bar Harbor, ME, USA) were bred in an approved bioresource unit at Dublin City University.

Antibodies and other reagents

Rabbit affinity-purified polyclonal antibodies specific for dynamin 1, 2, or 3 were bought from Acris Antibodies (Herford, Germany); monoclonals anti-dynamin 1 or 2, anti-Amph2, anti-clathrin light chain, and Pitstop 2 and its negative control from Abcam (Cambridge, UK); rabbit Amph1 polyclonal, a monoclonal antibody to an intralumenal epitope of synaptotagmin I (Syt-ecto), and rabbit VAMP2 polyclonal from Synaptic Systems (Goettingen, Germany); Amph1 mouse monoclonal from Santa Cruz Biotechnology (Heidelberg, Germany); goat anti-rabbit Alexa-594 and -488 or goat anti-mouse Alexa-594 and -488 from Jackson ImmunoResearch (Hamburg, Germany); mouse TrueBlot HRP secondary antibody from eBioscience (Hatfield, UK); clathrin HC mouse monoclonal (clone TD.1), IgG fraction of rabbit antiserum against AP2α2, affinity-isolated rabbit anti-β-tubulin III, monoclonal for syntaxin 1, dynasore, protein A agarose, and short-hairpin (sh)RNA lentiviral transduction particles, and nontargeted PLK0.1-puro control transduction particles from Sigma (Arklow, Ireland); bafilomycin A1 (Baf A1) from LC Laboratories (Woburn, MA, USA); protease inhibitor cocktail from Calbiochem (Nottingham, UK); Duolink proximity ligation assay (PLA) reagents (red fluorescence detection) from

Olink Bioscience (Uppsala, Sweden); and microdishes from Ibidi (Martinsried, Germany). Nicked chimera EA and BoNT/A were prepared recombinantly and characterized as described previously (29, 30).

Construction, expression, and purification of recombinant BoNT/B wild-type (WT) and its mutant

Experimentation on recombinant BoNTs has been approved by the Environmental Protection Agency of Ireland and performed under containment level 2. The synthetic gene encoding BoNT/B was cloned into a modified pET29a vector that contains a thrombin cleavage site for removal of the C-terminal His_6 tag (31). Subsequently, extra nucleotides were also added into the loop region to encode a thrombin consensus site for nicking (31). To abolish the interaction of BoNT/B with its protein acceptor, nucleotides encoding Ala at position 1196 were mutated to those encoding Lys by site direct mutagenesis to yield a construct encoding mutant BoNT/B (MT; A1196K; ref. 13). BoNT/B and MT were expressed in BL21.DE3 strain and purified by immobilized metal affinity chromatography (29). After being nicked with thrombin (1 U/mg of BoNT for 1 h at 22°C), phenylmethylsulfonyl fluoride was added to a final concentration of 1 mM to stop the protease action.

Culturing of primary neurons, transfection, and treatment with inhibitors of endocytosis

CGNs and TGNs were isolated from rats or mice and cultured as before (29, 32). Rat CGNs were incubated with 80 μM of dynasore (in 0.8% DMSO) for 1 h before exposure to 0.5 nM chimera EA or BoNT/A or 10 nM BoNT/B under basal or K^+ stimulation condition, in the continued presence of dynasore for 5 min; this was followed by 3 washes and incubation in basal medium (plain DMEM) containing dynasore for the times indicated before being harvested for detection of SNAP-25 or VAMP2 cleavage. In certain experiments, Baf A1 (100 nM) was applied to the cells 1 h before and during measurement of toxin internalization. To impair clathrin function, Pitstop 2 or its negative control (which has a closely related structure) was added for 5 min to the cultured neurons before their exposure to EA in the presence of Pitstop 2 or negative control and all the steps (thereafter) before assaying uptake.

Assay of the endocytosis of BoNTs

Quantitation of the uptake of BoNT/A, chimera EA, or BoNT/B into neurons was based on their cleavage intracellularly of SNAP-25 or VAMP2. As CGNs are more sensitive to BoNTs than TGNs, 0.5 nM EA or BoNT/A (for CGNs, 5 min) or 10 nM of either toxin (for TGNs, 10 min) was applied at 37°C in K^+ stimulation buffer (mM: 20 HEPES, 55 NaCl, 70 KCl, 2 $MgCl_2$, 1.3 $CaCl_2$, and 5 glucose) for CGNs and for TGNs (mM: 22.5 HEPES, 78.5 NaCl, 60 KCl, 1 $MgCl_2$, 2.5 $CaCl_2$, 3.3 glucose, and 0.1% BSA, pH 7.4), or basal (3.5 mM K^+) buffer with appropriate adjustments of NaCl (29, 32). Ca^{2+}-independent internalization of EA was determined using the same buffers except omitting Ca^{2+} and including 3 mM EGTA. After uptake of BoNTs, cells were washed 3 times with basal buffer, followed by incubation in basal fresh medium for the times indicated before being quantified SNAP-25 cleavage by SDS-PAGE and Western blotting (30). For EA and BoNT/A, the percentage of cleaved SNAP-25 was calculated relative to the total (*i.e.*, cleaved and uncleaved); in the case of BoNT/B, VAMP2 cleavage was normalized according to a loading control (SNAP-25) before analysis relative to the untreated control cells.

KD of dynamins, clathrin, AP2α2, or Amph1 with shRNAs

At 7 d in culture, CGNs or TGNs from mice were incubated in medium containing shRNA lentiviral particles that specifically target dynamin 1, 2, or 3, HC of clathrin, AP22, or Amph1, or nontargeted PLK0.1-puro control particles (400 transducing units/well), and cultured as above. After 7–10 d, chimera EA was applied as specified earlier in K^+-depolarization buffer, washed with basal buffer, and incubated in fresh basal medium for 30 min (a time at which no cleavage of SNAP-25 was observed under resting conditions) before Western blot analysis of protein KD and SNAP-25 proteolysis. The specific KD of each isoform of dynamin without off-target effects was also established by Western blotting the treated samples, using the other 2 isoform-specific antibodies. KD of each protein (%) was calculated relative to nontreated control. SNAP-25 cleavage (% total, *i.e.*, cleaved and uncleaved) was determined as above. For calculating the percentage inhibition of the cleavage after KD, SNAP-25 cleavage for shRNA-treated neurons was subtracted from the value obtained for control cells; the resultant number was expressed relative to that of the control.

Targeted genes/protein IDs and validated sequences for shRNA lentiviral transduction particles were as follows: NM_007459, AP2α2: CCGGGTGAACTGATCCGGTTGATTACTCGAGTAATCAACCGGATCAGTTCACTTTTTG; NM_001003908, clathrin HC: CCGGCTGAACAAATACGAGTCCTTACTCGAGTAAGGACTCGTATTTGTTCAGTTTTTG; NM_010065, dynamin 1: CCGGCCTGCGACATTCTATAAATATCTCGAGATATTTATAGAATGTCGCAGGTTTTTG; NM_007871, dynamin 2: CCGGGCCCGCATCAATCGTATCTTTCTCGAGAAAGATACGATTGATGCGGGCTTTTTG; NM_172646, dynamin 3: CCGGCCCACTATAATCCGTCCACTACTCGAGTAGTGGACGGATTATAGTGGGTTTTTG; and NM_175007, Amph1: CCGGGCAGTCATCATTCCTGCCTTTCTCGAGAAAGGCAGGAATGATGACTGCTTTTTG.

Competition binding assay

GST or GST–SV2C luminal domain 4 (SV2C-L4) (5 μM; refs. 7, 33) was premixed with 500 pM EA in basal or K^+-stimulation buffer for 30 min at 4°C. The mixture was applied to CGNs for 5 min at 37°C before being washed 3 times using fresh basal medium. Cells were further incubated for the times indicated before being harvested for SNAP-25 cleavage assay.

Monitoring membrane trafficking and cytochemical staining

TGNs on coverslips were incubated for 10 min at 37°C in 0.5 ml of K^+-stimulation buffer with or without Syt-ecto (1:100) before being washed and fixed. For immunostaining dynamin isoforms and/or Amph1, samples were washed, fixed, permeabilized, and blocked as before (32). Primary antibodies were applied in the blocking solution for 1 h at room temperature; after washing, fluorescent secondary antibodies were added for 1 h. To quantify the extent of colocalization, images were converted to 16-bit grayscale and analyzed by Pearson's correlation coefficient, using ImageJ 1.37a (U.S. National Institutes of Health, Bethesda, MD, USA). For live-cell imaging, the cells on microdishes were transfected with SypHluorin and cultured for 7 d, treated with or without dynasore (80 μM) for 1 h before being imaged with a Zeiss LSM 710 confocal microscope (Carl Zeiss, Oberkochen, Germany). Data analysis was carried out with ZEN software (Universal Imaging, Göttingen, Germany), using the time-lapse mode;

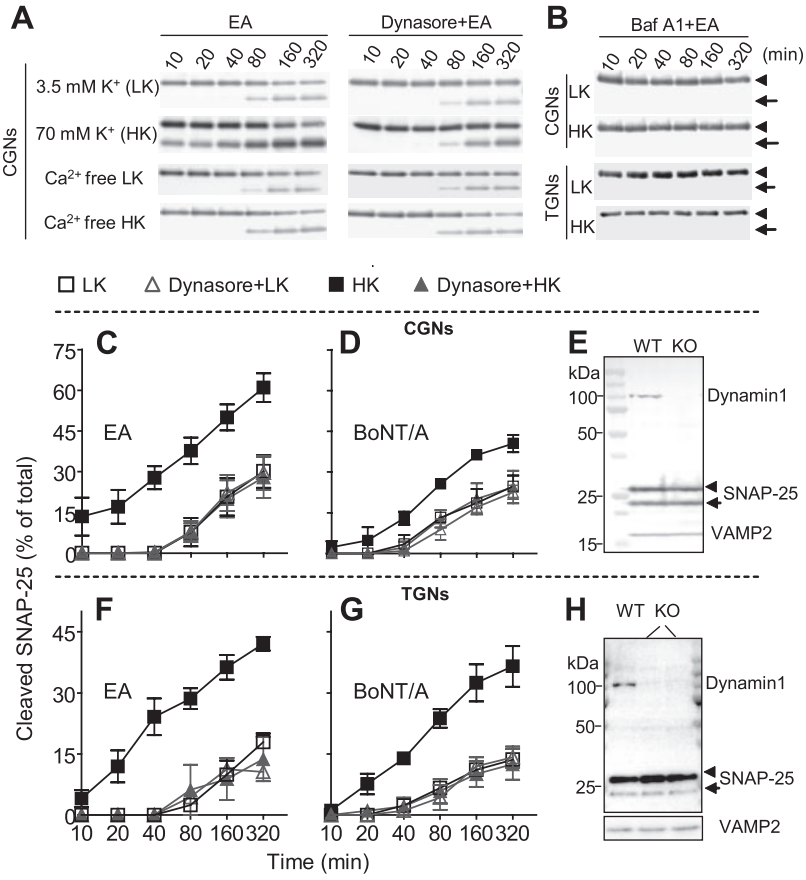

Figure 1. Dynamins in CGNs and TGNs do not participate in the basal uptake of BoNTs but are used for activity-dependent internalization: both processes require acidified compartments. Rat neurons were preincubated with 80 μM dynasore or its vehicle before being exposed for 5 or 10 min, respectively, at 37°C in LK or HK, to 0.5 nM (CGNs) or 10 nM (TGNs) BoNT/A or EA. After being washed, the cells were incubated for the specified times before Western blotting with an antibody recognizing both intact (arrowheads) and truncated (arrows) SNAP-25. *A*) Representative blots. *B*) Baf A1 (100 nM) abolished resting and evoked internalization of EA into both cell types. *C–H*) Quantified SNAP-25 cleavage showed that dynasore inhibited the evoked but not resting entry of EA (*C*, *F*) and BoNT/A (*D*, *G*) into CGNs (*C*, *D*) or TGNs (*F*, *G*). Values are means ± SE; $n \geq 3$. *E*, *H*) CGNs (*E*) or TGNs (*H*) from a litter of WT or dynamin-1-KO mice were treated with 0.5 nM EA (*E*) or 10 nM EA (*H*) for 5 min (*E*) or 10 min (*H*) in LK, followed by washout and postincubation in fresh basal medium for 320 min. Expression of dynamin 1 and cleavage of SNAP-25 were analyzed by Western blotting. VAMP2 served as an internal loading control. Representative blots show that neither dynamin-1-KO CGNs nor TGNs showed reduced basal uptake of EA.

changes in intensity of the fluorescent spots in regions of interest, *i.e.*, active boutons, were calculated by subtracting the average signal before stimulation (F_0) from the higher values obtained after depolarizing the cells (F).

Coimmunoprecipitation of dynamin and Amph isoforms

Murine cultured TGNs or CGNs were incubated in K^+-stimulation buffer for 10 or 5 min, respectively, before centrifugation for 5 min at 170 *g*; cell pellets were lysed in HEPES (20 mM, pH 7.4) containing 150 mM NaCl, 1 mM MgCl, 1 mM EGTA, and 0.1% Triton X-100 supplemented with a cocktail of protease inhibitors for 30 min, followed by brief sonication. After centrifugation at 15,000 *g* for 10 min, the protein concentration of the supernatant was determined by Bradford's assay. Protein extracts (100 μg in 100 μl) were incubated with dynamin isoform-specific rabbit antibodies (10 μg in 50 μl), precomplexed with protein-A agarose for 1 h, before being washed 5 times with lysis buffer. Negative controls were performed using rabbit nonimmune IgG and prelabeled protein A agarose. Before and after binding, 10 μl samples of input and unbound were kept for analysis of the efficiency of coimmunoprecipitation. The sealed agarose-bound samples were boiled for 10 min in 50 μl reducing LDS sample buffer before 50% of the eluate was subjected to SDS-PAGE and Western blotting, using mouse monoclonal antibodies specific for Amph1 or 2 and mouse TrueBlot HRP secondary antibody.

In situ PLA

Cultured CGNs and TGNs from Thy1-YFP mice were stimulated by K^+-depolarization for 5 min before fixation, permeabilization, blocking, and incubation with primary antibodies (monoclonals for either dynamin 1 or 2, 1:1000; and rabbit polyclonal against Amph1, 1:500). PLA was carried out according to the manufacturer's instructions. Negative controls were performed likewise, except for omitting one or other of the primary antibodies. Images were taken using the confocal microscope.

Statistical analysis

Probability values were determined with the use of Student's 2-tailed *t* test. Values of $P < 0.05$ were considered significant.

RESULTS

Basal entry of BoNTs into both glutamatergic and peptidergic neurons requires protein acceptors and acidified compartments but not dynamins

Experiments largely utilized a BoNT chimera, EA, containing the translocation and protease domains from BoNT/E but the acceptor binding moiety of BoNT/A (29). It offers the advantages of a faster internalization and more extensive cleavage of intracellular SNAP-25 than BoNT/A; moreover, TGNs are more susceptible to EA than BoNT/E (33). BoNT/A, /B, and /E were used for comparison where appropriate. CGNs and TGNs were briefly (5 and 10 min) exposed to EA (0.5 and 10 nM, respectively) in low-K^+-concentration (LK) buffer with or without Ca^{2+}, washed, and incubated in fresh medium for the times indicated (**Fig. 1*A*,**

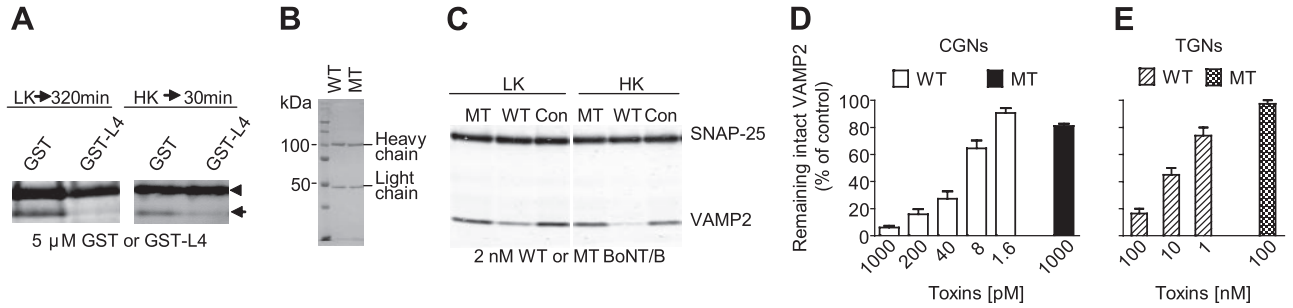

Figure 2. Basal and K^+-stimulated entry into CGNs or TGNs of BoNT EA and BoNT/B involve binding to their respective protein acceptors. *A*) GST or GST-SV2C-L4 (5 μM) was premixed with 0.5 nM chimera EA in LK or HK for 30 min at 4°C before addition to rat CGNs for 5 min at 37°C. Toxins were washed away with fresh basal medium before postincubation for 320 min (for LK) and 30 min (for HK). Arrowhead and arrow indicate the intact and cleaved SNAP-25, respectively. *B*) SDS-PAGE analysis of purified WT and MT (known to have greatly reduced ability to bind its protein acceptor) in the presence of 50 mM DTT followed by Coomassie staining. *C*) CGNs were exposed to 2 nM BoNT/B WT or MT in LK or HK for 10 min before brief washing and further incubation for 24 h, followed by Western blotting for VAMP2. SNAP-25 was used as internal loading control. Con, nontoxin-treated control. *D, E*) CGNs (*D*) or TGNs (*E*) were treated with BoNT/B or MT for 24 h at 37°C without stimulation before Western blotting. Intact VAMP2 remaining was calculated relative to that in nontoxin-treated control, using SNAP-25 as internal loading control. Values are means ± SE; $n = 3$.

C, F). Cleavage of SNAP-25 in both cell types, quantified by Western blotting, revealed significant time-dependent basal uptake of this toxin after a lag of >40 min (Fig. 1*A*, *C*, *F*). Similar findings were obtained when the CGNs and TGNs were exposed in LK to BoNT/A (0.5 and 10 nM, respectively; Fig. 1*D*, *G*), suggesting that the same activity-independent mechanism is exploited by both EA and BoNT/A. Evidence that EA passes through an acidic compartment was obtained by pretreating each cell type with an inhibitor of vH^+-ATPases to block acidification of endocytotic vesicles. Inclusion of Baf A1 (100 nM) for 1 h beforehand, and throughout the experiments, abolished the resting toxin translocation (in LK) into cytosol, as reflected by an absence of SNAP-25 cleavage (Fig. 1*B*). BoNT/A and /B gave the same pattern of results (not shown).

To ascertain whether dynamins are involved in the basal entry, their GTPases were inactivated with 80 μM dynasore (34) by preincubation of CGNs and TGNs for 1 h (and throughout the experiments); this proved ineffective on the resting uptake of EA in either cell type (Fig. 1*A*, *C*, *F*). In the case of BoNT/A, basal uptake was likewise unaffected by dynasore (Fig. 1*D*, *G*). Similar findings were also obtained with dynasore for BoNT/E and /B on CGNs (Supplemental Fig. S1*A*, *B*). Use of an available dynamin-1-KO mouse established that the basal entry of BoNT EA into CGNs or TGNs was unaffected (Fig. 1*E*, *H*).

As the basal uptake of the toxins does not involve dynamins, it became important to ascertain whether this process requires protein acceptors. Preincubation of chimera EA with SV2C-L4, its acceptor, reduced the basal uptake by CGNs; this was evident from the decreased cleavage of SNAP-25 by the GST-SV2C-L4 fusion but not by GST alone (**Fig. 2*A***). In the case of BoNT/B, this question was addressed by preparing a mutant (MT) containing an altered single residue (A1196K) in the C-terminal region of its HC that is known to be essential for binding to the protein acceptor synaptotagmin (13). A fixed concentration of recombinantly expressed and purified BoNT/B MT (Fig. 2*B*) failed to internalize into CGNs under basal conditions, as reflected by the lack of VAMP2 cleavage, whereas the WT BoNT/B cleaved ~45% VAMP2 (Fig. 2*C*). A similar outcome was obtained when varied concentrations of WT or MT were incubated with CGNs or TGNs (Fig. 2*D*, *E*). Therefore, for the first time, it is established that basal uptake of BoNTs into CGNs and TGNs involves binding to protein acceptors, uptake *via* acidic compartments and eventual translocation to their cytosolic site of action.

Depolarization of CGNs and TGNs recruits dynamin-dependent endocytosis and augments BoNT uptake

Consistent with SV2 being the acceptor for BoNT/A and EA that mediates their uptake (see introduction), depolarization in the presence of Ca^{2+} promoted their neuronal internalization. Exposure of CGNs or TGNs to (0.5 or 10 nM) EA in high-K^+-concentration (HK) buffer for 5 or 10 min, respectively, followed by incubation in basal medium increased the internalization of EA, as revealed by an earlier onset and more extensive cleavage of SNAP-25 than in LK or Ca^{2+}-free solutions (Fig. 1*A*, *C*, *F*). Likewise, K^+-depolarization of CGNs and TGNs raised the uptake of BoNT/A (Fig. 1*D*, *G*) and BoNT/E or /B in CGNs (Supplemental Fig. S1*A*, *B*); the latter were not tested in TGNs because of their low activity in these neurons (32, 33). As expected, the evoked uptake of EA and BoNT/B by CGNs was blocked by inhibiting their interaction with respective protein acceptors (Fig. 2*A*, *C*). Again, Baf A1 prevented the cleavage of SNAP-25 by EA (Fig. 1*B*) and by BoNT/A or /B (unpublished results) in the depolarized cells, confirming their trafficking through acidified compartments. Inhibition of the evoked uptake of EA and BoNT/A, /E, and /B to the basal level was seen with 80 μM dynasore in CGNs (Fig. 1*A*, *C*, *D* and

Supplemental Fig. S1*A*, *B*), an effect reversed by drug washout (not shown), revealing an absolute requirement for dynamins in this activity-evoked process. Similar findings were made in TGNs exposed to EA and BoNT/A (Fig. 1*F*, *G*). Hence, depolarization-elicited internalization of BoNTs by neurons mostly containing either SCSVs or LDCVs depends on dynamins, unlike the resting uptake.

Evoked internalization of EA by neurons also involves clathrin and AP2

As dynamin can support endocytosis by either clathrin-dependent or -independent mechanisms (reviewed in refs. 35, 36), it was pertinent to establish whether clathrin is required for the entry of the toxins. For this purpose, SNAP-25 cleavage was measured 30 min after toxin washout, a time when only evoked internalization was detectable (*cf.* Fig. 1*C*, *F*). In CGNs, KD of clathrin HC by shRNA produced a large, proportionate decrease in the HK-induced uptake of EA, as reflected by a reduction in cleavage of SNAP-25 (**Fig. 3*A, B***). Accordingly, AP2 was also found to be essential. KD of AP2α2 subunit in CGNs resulted in a severe blockade of SNAP-25 cleavage by EA (Fig. 3*C*, *D*). As similar KD of clathrin in TGNs proved unsuccessful, a pharmacological approach was adopted to specifically block clathrin-mediated endocytosis. Inclusion of Pitstop 2 (37) together with EA during K^+-depolarization and the subsequent incubation in toxin-free medium yielded a significant reduction of SNAP-25 cleavage in TGNs (Fig. 3*E*, *F*), like CGNs (Supplemental Fig. S1*C*); this effect was specific because an inactive analog gave no such decrease. In summary, the evoked neuro-endocytosis of EA chimera involves dynamin, clathrin, and AP2.

Different dynamin isoforms are utilized in evoked endocytosis of BoNT by neurons containing mostly SCSVs or LDCVs

All dynamin isoforms contribute to the uptake of BoNT by glutamatergic CGNs but to different degrees

Western blotting with antibodies specific for each dynamin isoform revealed that CGNs express all 3 dynamins (**Fig. 4*A***). Involvement of individual dynamins in the stimulated internalization of BoNT was examined by selective KD of each variant, as well as taking advantage of dynamin-1-KO mice. In the requisite shRNA-treated CGNs from WT mice, the average levels of dynamin 1, 2, and 3 were significantly reduced compared with the untreated controls (Fig. 4*B*). Each isoform was selectively reduced without any alternation in the others (Supplemental Fig. S2*A*); also, no change was seen in a negative control treated with nontargeted lentiviral particles (Supplemental Fig. S2*B*). The detection of 2 immunoreactive bands for dynamin 2 in CGNs (Supplemental Fig. S2*A*) might reflect the expression of splice variants, as reported previously (38, 39), but this notion was not pursued here. KD of dynamin 1, 2, and 3 reached ~94, ~66, and ~76%, which was accompanied by inhibition of EA uptake and cleavage of SNAP-25 by ~42, ~55, and ~21% (Fig. 4*B*). Thus, all 3 dynamins contribute to the endocytosis of EA, although to dissimilar extents. Likewise, CGNs from dynamin-1-KO mice showed a substantial reduction (~48%) of EA uptake relative to WT (Fig. 4*C* and Supplemental Fig. S2*C*), approximating to the value obtained by dynamin 1 KD (Fig. 4*B*). Secondary KD of dynamin 2 (~65%) in CGNs prepared from dynamin-1-KO mice resulted in an ~70% inhibition of activity-dependent uptake of EA relative to WT, equivalent to 22% additional blockade over the KO value (Fig. 4*C* and Supplemental Fig. S2*D*). This composite figure represents

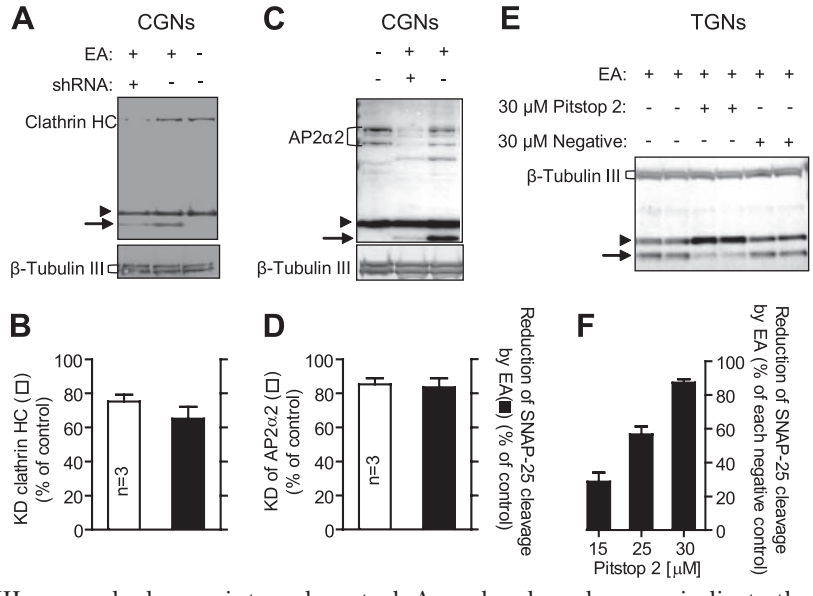

Figure 3. KD of clathrin HC or AP2α2 inhibited depolarization-dependent uptake of EA by CGNs: Pitstop 2 reduced the evoked entry into TGNs. *A–D*) Murine cultured CGNs were treated with or without shRNA targeting clathrin HC (*A*, *B*) or AP2α2 (*C*, *D*) before 5 min exposure to EA in HK, followed by washing and 30 min incubation in basal medium before Western blotting. Decreases in the expression of each target protein and SNAP-25 proteolysis were monitored simultaneously using the requisite antibodies. *E*) TGNs were incubated with Pitstop 2 or its negative control for 5 min before their further incubation with EA for 10 min in HK. Neurons were then washed and incubated for 30 min in basal medium containing drug or its control before quantification of SNAP-25 cleavage. *F*) Decreased cleavage by EA in the presence of Pitstop 2 was calculated relative to that in toxin-treated cells exposed to the equivalent concentration of an inactive analog. Values are means ± SE; $n = 3$. β-Tubulin III was probed as an internal control. Arrowheads and arrows indicate the intact and cleaved SNAP-25, respectively.

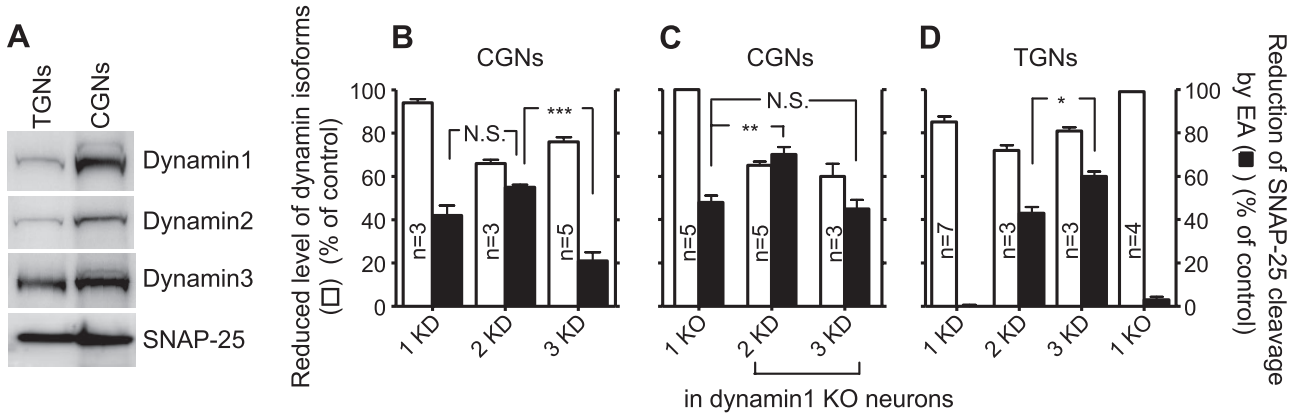

Figure 4. Activity-dependent endocytosis of EA utilizes dynamin 1 in CGNs but not TGNs: dynamin isoforms make distinct but overlapping contributions. *A*) Western blots of equivalent amounts of total cell lysate from CGNs and TGNs, with dynamin isoform-specific antibodies. SNAP-25 was probed as internal control. *B*) Mouse CGNs treated with or without shRNA specific for dynamin isoforms were incubated with 0.5 nM EA, for 5 min in HK, followed by washout and incubation in fresh basal medium for 30 min. KD of each isoform and reduction of SNAP-25 cleavage by EA relative to control were calculated (see Materials and Methods). *C*) CGNs from the dynamin-1-KO mice showed a reduced level of stimulated EA uptake. KD of isoform 2 further decreased EA entry into dynamin-1-KO CGNs, whereas no significant change was observed with KD of isoform 3. *D*) In TGNs, neither KD nor KO of dynamin 1 significantly reduced stimulated EA uptake, whereas KD of either isoform 2 or 3 reduced EA endocytosis but to different extents. Data represent means ± SE; *n* values are plotted. Representative Western blots for above are shown in Supplemental Fig. S2 (CGNs) and S3 (TGNs). N.S., nonsignificant ($P>0.05$). *$P< 0.05$; **$P< 0.01$; ***$P< 0.001$.

incomplete additivity of the extents of inhibition of uptake in dynamin 1 KO or isoform 2 KD. Hence, these 2 isoforms seem to make separate but, also, some overlapping contributions to the stimulated endocytosis of EA. In contrast, ~60% KD of dynamin 3 in dynamin-1-KO CGNs failed to further reduce this EA uptake (Fig. 4*C* and Supplemental Fig. S2*E*).

Endocytosis of BoNT by peptidergic sensory neurons uses dynamin 2 and 3, but not 1

Three isoforms of dynamin were also detected in cultured TGNs (Fig. 4*A*); notably, the approximate ratios of dynamin 1, 2, and 3 between CGNs and TGNs were calculated to be ~6.0, 2.4, and 1.1, respectively. KD of dynamin 1 in TGNs was achieved without altering the levels of isoform 2 or 3 (Supplemental Fig. S3*A*). Despite a KD of ~85%, this failed to exert any detectable effect ($n=7$) on activity-dependent EA endocytosis (Fig. 4*D*). Likewise, KO of dynamin 1 caused no significant reduction of EA uptake (Supplemental Fig. S3*B* and Fig. 4*D*). In contrast, substantial drops in SNAP-25 cleavage (~43 and ~60%) resulted from the specific KD of dynamin 2 or 3 (Fig. 4*D*), without affecting other isoforms (Supplemental Fig. S3*A*); control viral particles failed to inhibit EA uptake (Supplemental Fig. S3*C*).

Differences in the dynamins participating in endocytotic processes exploited by BoNT to enter CGNs and TGNs also revealed by functional assays of the retrieval of vesicle proteins

Synaptotagmin I is a Ca^{2+} sensor for exo/endocytosis (40) that is expressed on both SCSVs and LDCVs (32, 41). It is known to undergo dynamin- and activity-dependent endocytosis (42). Syt-ecto is a useful probe for exo/endocytosis (43). TGNs were exposed for 10 min to HK to elicit the transfer of synaptotagmin I to the plasmalemma and, thereby, enhance the binding of an Oyster 550-tagged Syt-ecto IgG. Accordingly, Syt-ecto brightly labeled TGNs under stimulated (**Fig. 5*A***) but not basal conditions (Fig. 5*B*). Subsequently, the stimulated cells were washed, fixed, and permeabilized before costaining with antibodies selective for dynamin isoforms. Imaging of the red fluorescence revealed punctate staining with Syt-ecto of neuronal fibers (Fig. 5*C–E*), reflective of areas of exo/endocytosis. Moreover, all the dynamins yielded a similar labeling pattern (Fig. 5*C–E*). Calculation of Pearson's correlation coefficients (Fig. 5*F*) established colocalization of Syt-ecto with dynamin 2 and 3, implicating both in exo/endocytosis. In contrast, the poor spatial correspondence between Syt-ecto and dynamin 1 mitigates against its participation.

Advantage was taken of SypHluorin as a probe for real-time microscopic imaging of exo/endocytosis in live neurons (44); the intensity of the green fluorescent signal increases on exocytosis and becomes quenched when endocytosed into acidic compartments. In TGNs transfected with SypHluorin, HK triggered a robust increase of fluorescence above the baseline in LK, followed by a decay over ~150 s to background level (Fig. 5*G*). The latter is attributable to trafficking into acidic endosomes because the loss of fluorescence was prevented by inhibiting the vH^+-ATPase pump with Baf A1 (unpublished results). In accord with the lack of inhibition of EA uptake by KO of dynamin 1 (*cf.* Figure 4*D*), ablating this isoform did not delay fluorescence decay in TGNs (Fig. 5*G*). A contrasting severe delay induced by dynasore of fluorescence quenching impli-

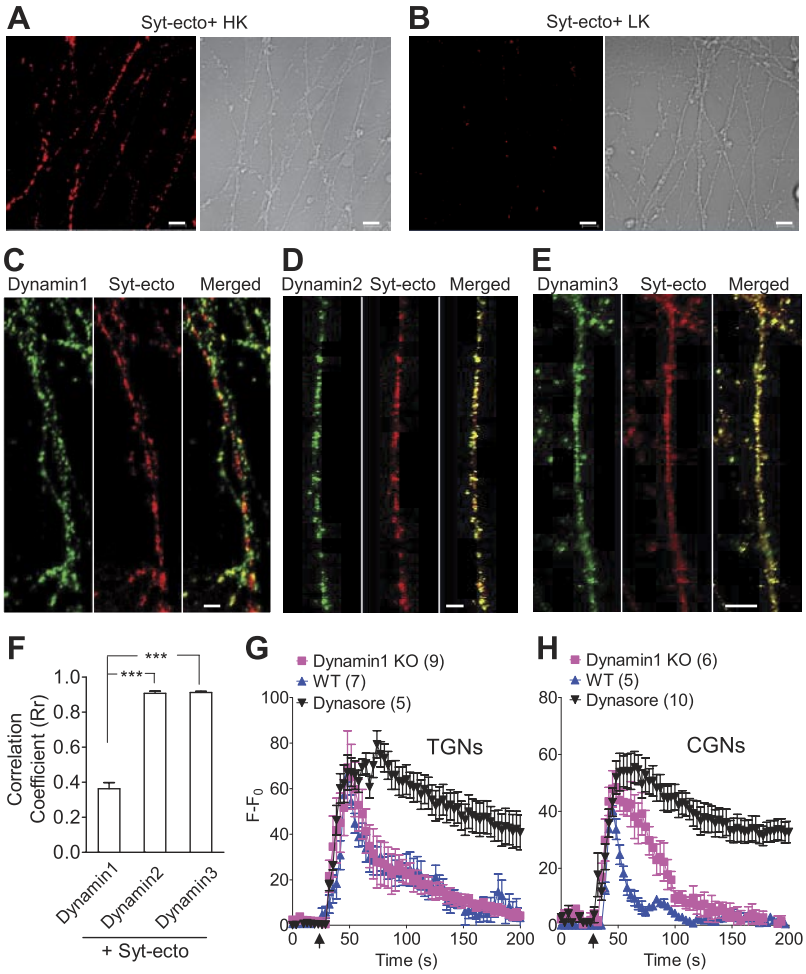

Figure 5. Dynamin 1, unlike other variants, does not colocalize with Syt-ecto in HK-stimulated TGNs, and is not required for evoked SypHluorin endocytosis, in contrast to CGNs. *A*, *B*) Rat TGNs were incubated with Syt-ecto for 10 min in HK (*A*) or LK (*B*) before washing and fixation. Confocal images show that Syt-ecto brightly labeled the stimulated (*A*) but not the nonstimulated neurites (*B*). *C–E*) Rat TGNs were pretreated with Syt-ecto for 10 min in HK before washing, fixation, permeabilization and incubation with dynamin antibodies. Representative images show that dynamin 1 (*C*, green) displayed minimal codistribution with Syt-ecto (*C*, red) on the neurites, in contrast to the striking colocalization with Syt-ecto (yellow) observed for dynamin 2 (*D*, green) and 3 (*E*, green). Scale bars = 5 μm. *F*) Pearson's correlation coefficient analysis was used to compare the colocalization level of dynamin isoforms with Syt-ecto; bars are means ± SE; $n \geq 3$ independent cultures. *G*, *H*) Fluorescence changes in arbitrary units (F–F_0) induced by K^+-stimulation of SypHluorin-expressing TGNs from WT or dynamin-1-KO mice (*G*) or CGNs (*H*) in the absence or presence of dynasore. HK was added at ~30 s, as indicated by arrows. Values are means ± SE; n indicates the number of cells recorded from ≥4 independent cultures. $^{***}P < 0.001$.

cates dynamin 2 and 3 in the endocytosis of SypHluorin (Fig. 5*G*). In SypHluorin-expressing CGNs, stimulation evoked a similar rise in fluorescence, but the decay profile was somewhat different; there was a faster initial decline in the fluorescence followed by a small peak (Fig. 5*H*). Thus, CGNs apparently exhibit a fast phase of endocytosis that was not seen in TGNs. Notably, KO of dynamin 1 delayed or slowed decay of the fluorescence of SypHluorin (Fig. 5*H*); presumably, isoform 1 mediates the fast phase of endocytosis, while isoforms 2 and 3 support the slower retrieval, a notion supported by the more extensive delay in cells exposed to dynasore (Fig. 5*H*).

Distinct utilization of Amph1 and 2 for evoked entry of BoNT into CGNs and TGNs

Amph1 and 2 are present in CGNs, but TGNs contain only isoform 1, which is required for toxin internalization and colocalizes with dynamin 2

On neuronal stimulation, dynamins are recruited to endocytotic sites *via* binding to Amphs (45, 46); thus, the presence of the latter was sought in both neuron types. Western blotting with antibodies selective for Amph1 or 2 revealed that CGNs contain each but only isoform 1 could be detected in TGNs (**Fig. 6*A***). Substantial KD (~75%) of Amph1 in CGNs did not reduce the evoked EA uptake, as shown by a failure to inhibit SNAP-25 cleavage (Fig. 6*B*); as it proved impractical to KD isoform 2, its contribution to toxin uptake could not be established directly. In the case of TGNs, KD of Amph1 was incomplete (~55% reduction) but still resulted in a significant decrease in evoked uptake of EA (by ~30%; P=0.006 compared with control; Fig. 6*B*). Accordingly, stimulation of TGNs followed by fixation, permeabilization, and incubation with the requisite antibodies resulted in labeling of Amph1 in cell bodies and fibers (Fig. 6*C*, *D*). Counterstaining with dynamin isoform-specific monoclonal IgGs (Fig. 6*C*, *D*) visualized predominant colocalization of Amph1 with dynamin 2, quantified by use of Pearson's correlation coefficient (Fig. 6*E*, *F*). Such colocation extends the evidence for this pair of proteins contributing to endocytosis.

Both Amph isoforms in CGNs interact with all the dynamins, whereas in TGNs, Amph1 associates with dynamin 2 and 3, consistent with their proximities observed in situ

In stimulated CGNs, the 3 dynamins were shown to complex with both Amphs by immunoisolation on immobilized antibodies specific for each dynamin (**Fig. 7*A***);

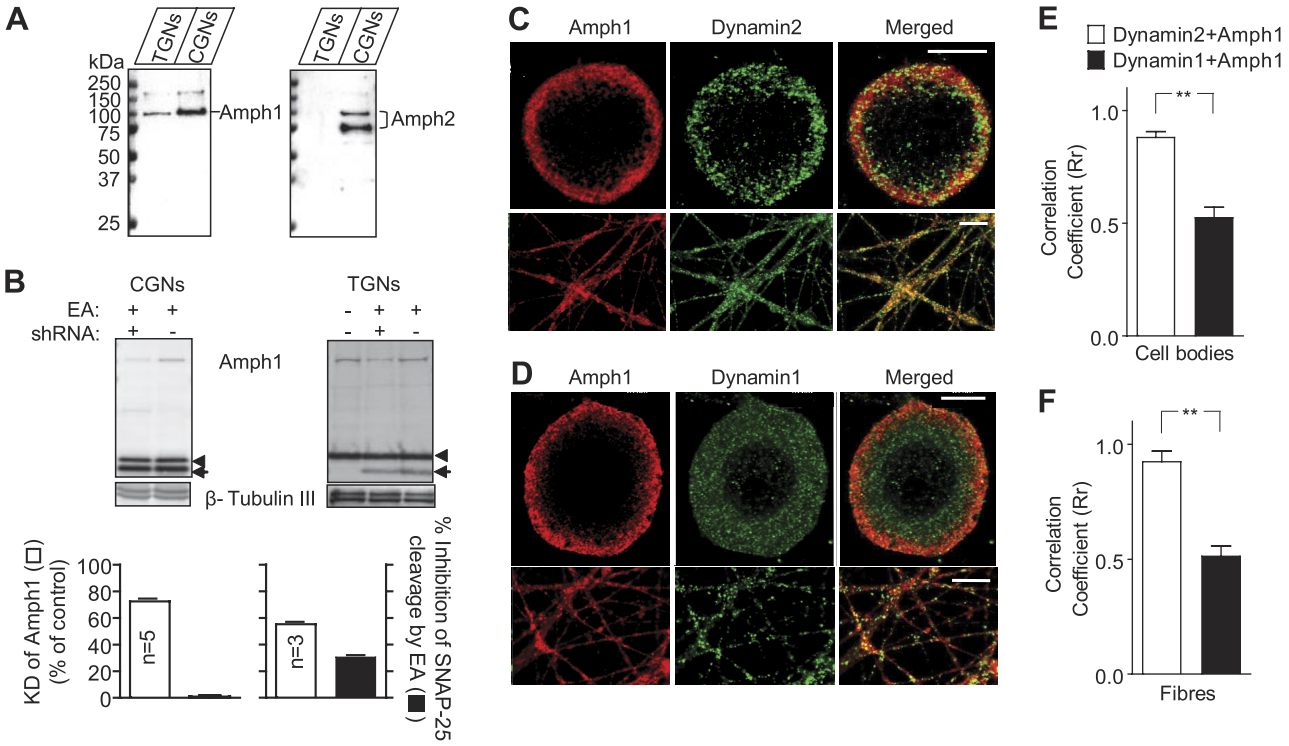

Figure 6. CGNs express both Amph isoforms, while TGNs contain only Amph1, which is colocalized with dynamin 2 but not 1: KD of Amph1 reduced evoked EA uptake by TGNs but not CGNs. *A*) Immunoblotting of the equivalent amounts of protein with isoform-specific antibodies revealed the expression of Amph1 and Amph2 in CGNs but only isoform 1 in TGNs. *B*) Mouse CGNs or TGNs treated with shRNA specific for Amph1 were incubated with 0.5 nM (for CGNs) or 10 nM (for TGNs) EA in HK, followed by washout and incubation in fresh basal medium for 30 min. Arrowheads and arrows indicate the intact and cleaved SNAP-25, respectively. β-Tubulin III was probed as internal control. Bottom panels indicate the extents of Amph1 KD and cleavage of SNAP-25 in tests and controls from simultaneous analysis, and calculated relative to shRNA-free controls. Values are means ± SE; *n* values are plotted. *C*, *D*) Confocal images of costaining on cell bodies and neurites for dynamin 2 and Amph1 (*C*) or dynamin 1 and Amph1 (*D*) in HK-stimulated TGNs; an appropriate, workable pair of antibodies for dynamin 3 and Amph1 could not be obtained. Scale bars = 10 μm. *E*, *F*) Pearsons' correlation coefficients were calculated to compare the colocalization level on cell bodies (*E*) and fibers (*F*), using images recorded from ≥5 independent experiments. Data are means ± SE; $n \geq 15$. $^{**}P < 0.01$.

selectivity of these associations was established by the lack of reactivity with nonimmune IgG. In accordance with the above-noted colocation of Amph1 and dynamin 2 in TGNs, these 2 proteins were found in complexes by their coisolation from extracts of the cultures, using dynamin isoform-specific IgGs prebound to protein A agarose. Western blotting showed that Amph1 interacts only with dynamin 2 and 3 (Fig. 7*B*); this might be partly due to the relative lower expression level of dynamin 1 in TGNs (Fig. 4*A*). As expected, isolation with dynamin antibodies failed to copurify Amph2 (Fig. 7*B*). This highlights another difference between exo/endocytosis in these sensory neurons containing LDCVs and CGNs possessing SCSVs, namely the former utilize Amph1-dynamin 2 or 3 complexes, unlike the latter in which their 3 dynamins associate with both Amph isoforms.

Evidence was accrued for these 2 proteins actually being adjacent inside neurons, using a sensitive and specific PLA. This utilizes a pair of antibodies, each having a complementary oligonucleotide attached. Only when the 2 IgGs bind to epitopes within 40 nm can the nucleotides be ligated to facilitate amplification; *in situ* visualization is achieved by labeling with fluor-tagged cDNA probes (47). It was advantageous to use neurons from Thy1-YFP mice (48) for background visualization of the neurons. In stimulated and subsequently permeabilized CGNs, probing for Amph1 and dynamin 1 or 2 yielded several fluorescent spots (average 15 on each) on the cell bodies (Fig. 7*C*); no significant difference existed between the number of signals seen when Amph1 was paired with dynamin 1 or 2 (Fig. 7*D*). Equivalent images were recorded for neurites (not shown). Labeling of TGNs for Amph1 (the isoform therein, see above) and dynamin 2 yielded a number of red spots in the neurites and soma (average 13/cell body; Fig. 7*E1*, *E3*, *F*); these were absent from controls lacking the dynamin (Fig. 7*E2*) or Amph1 antibody (not shown). In contrast, very few spots (<1/soma) resulted from labeling with IgG specific for dynamin 1 paired with that for Amph1 (Fig. 7*E4*, *F*). This established that Amph1 resides in proximity to dynamin 2, but not 1, in TGNs.

In summary, the Amphs and dynamins participating in stimulated, clathrin-mediated endocytosis of BoNT by sensory peptidergic TGNs have been identified, and use of distinct isoforms by CGNs revealed; dynamin 1 is required for the faster retrieval of SCSVs.

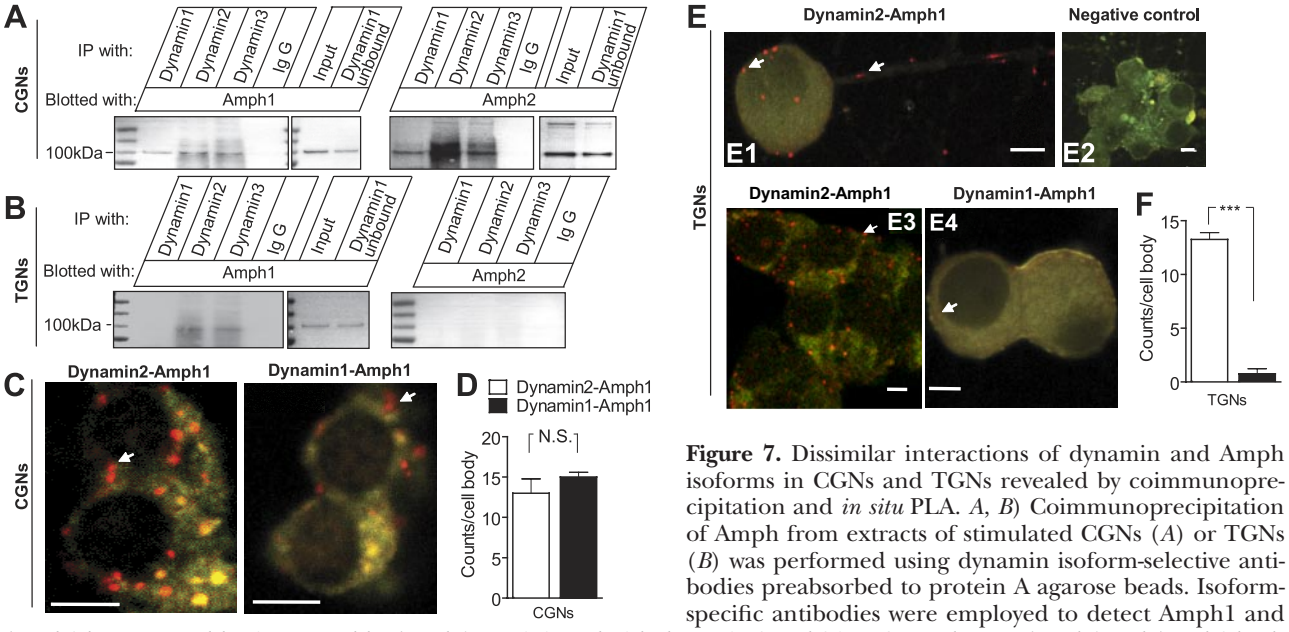

Figure 7. Dissimilar interactions of dynamin and Amph isoforms in CGNs and TGNs revealed by coimmunoprecipitation and *in situ* PLA. *A*, *B*) Coimmunoprecipitation of Amph from extracts of stimulated CGNs (*A*) or TGNs (*B*) was performed using dynamin isoform-selective antibodies preabsorbed to protein A agarose beads. Isoform-specific antibodies were employed to detect Amph1 and Amph2 by Western blotting. Notably, Amph1 precipitated with dynamin 2 and 3 in TGNs, whereas Amph1 and Amph2 both sedimented with all 3 dynamins in CGNs. An aliquot (10%) of input and unbound fractions from dynamin 1 antibody-protein A beads and eluate (50%) were subjected to Western blotting. Intensities of the bands were calculated using ImageJ; coimmunoprecipitation efficiency estimated for dynamin 1/Amph1 was ~8%, and dynamin 1/Amph2, ~10%, in CGNs. *C*) PLA shows that both dynamin 1 and dynamin 2 reside in proximity to Amph1 in CGNs. *D*) Positive signals for dynamin 1 and 2 with Amph1, calculated from the number of red spots on each cell body from 20 randomly selected CGNs, showed no significant difference in Students' *t* test. *E*) Dynamin 2 (*E1*, *E3*), in contrast to dynamin 1 (*E4*), was visualized in proximity to Amph1 in TGNs using the *in situ* PLA. *E2* represents the negative control in the absence of dynamin antibody. *F*) Discrete images of PLA in cell bodies of TGNs were counted and analyzed as outlined above for CGNs. Data show a significant difference between the levels of dynamin 1/Amph1 and dynamin 2/Amph1 interaction ($P<0.001$) in Students' *t* test. Arrows (*C*, *E*) exemplify positive fluorescent spots. Scale bars = 5 μm. Data are means ± SE from ≥3 separate experiments (*D*, *F*). $***P < 0.001$.

DISCUSSION

Substantial basal internalization of BoNT occurs in CGNs and TGNs involving protein acceptors and passage through acidic compartments but not dynamins

The discovery that synaptic vesicle proteins (in conjunction with gangliosides) serve as high-affinity acceptors for BoNTs (7, 13, 49) focused research on their activity-dependent uptake into nerves. In contrast, nonstimulated internalization of these proteins has received little attention but should not be disregarded (50). It has long been known that ^{125}I-labeled BoNT/A binds saturably to the presynaptic membrane of motor nerves in the absence of stimulation or extracellular Ca^{2+}, when azide is included to block its uptake (51). Moreover, the basal entry of toxin represents a substantial fraction (more than half) of the stimulated value in motor nerves (18) and was found herein to have slower onset than depolarization-elicited internalization of chimera EA in cultured CGNs. This may have consequences for both BoNT pathology and therapy (*e.g.*, by enabling at least some uptake into relatively quiescent nerves). The demonstrated requirement of binding of BoNT EA and /B to protein acceptors (SV2 and synaptotagmin, respectively) accords with acceptor-mediated internalization of radioiodinated BoNT/A and /B into motor nerve endings, as revealed by electron microscopy autoradiography (16, 51). Gangliosides act as coacceptors for BoNTs (7, 13, 49); inhibition of their synthesis prevents entry of BoNT/A into resting Neuro 2a or SK-N-SH cells (52). Consistent with our findings on motor nerve endings, briefly exposing TGNs or CGNs to BoNT/A or EA under resting conditions resulted in considerable (15–30%) cleavage of SNAP-25 after 5 h postincubation (*cf.* Fig. 1). The ability of a vH^+-ATPase inhibitor to prevent the latter/cytosolic translocation demonstrates involvement of an acidic compartment, implying trafficking *via* membrane-limiting organelles. Hence, SNAP-25 cleavage in resting neurons cannot be attributed to passive diffusion into any lysed cells, if present. Curiously, the basal uptake was not found to require dynamins even though they participate in the major endocytotic pathways mediated by clathrin or caveolae (35, 36). The latter are excluded due to being absent from neurons (35). Also, nonparticipation of clathrin was indicated by K^+-depletion, which disrupts its assembly into coated pits, failing to exert any inhibition (unpublished results). Few other modes of internalization fulfill the criteria identified herein for basal toxin uptake by neurons, except, for example, dynamin- and clathrin-independent carriers or

macropinocytosis (53). In this context, it is notable that there is convincing evidence for a dynamin-independent process in hippocampal organotypic slice cultures from FM dye and membrane capacitance measurements (54). Moreover, these authors showed that dynamin-independent and -dependent membrane recycling are independent processes linked to spontaneous and evoked exocytosis, respectively, similar to our findings with BoNT. The GM_1 ganglioside-binding B subunit of cholera toxin can also avail of dynamin-independent endocytosis in caveolin-1 null and WT mouse embryonic fibroblasts (55).

Activity/clathrin/Amph/dynamin-dependent endocytotic internalization of BoNTs into glutamatergic CGNs and peptidergic neurons

The increment in BoNT uptake induced in both cell types by depolarization was not due to a simple enhancement of the basal process but, rather, the triggering of an additional entry mode. This increases the toxin susceptibility of active nerves and, thereby, contributes to the preferential paralysis of motor nerves that underlies the pathogenic mechanism of botulism. Furthermore, such augmented entry of BoNT into the abnormal hyperactive nerves improves the clinical efficacy of BoNT injected locally (56). In relation to this, the elevated expression of neuronal SV2 in tissue biopsies from patients suffering with painful conditions (57) should contribute to the antinociceptive efficacy of Botox administered into the affected areas. Although BoNTs may initially bind with low affinity to gangliosides abundant on neurons, stimulation brings more synaptic vesicle protein acceptors to the surface by exocytosis. A resultant increase in high-affinity association with the dual acceptors enables the toxin to move into a faster endocytotic pathway (reviewed in ref. 58). In this context, it is noteworthy that SV2 isoforms contain tyrosine-based motifs that stimulate binding to AP2 (23, 59); this would then recruit the latter protein into clathrin-mediated endocytosis. Moreover, SV2 binds directly to Amphs (59); their interaction with clathrin, AP2, and dynamins would bring the acceptor with bound toxin to the CCPs for internalization, as recently observed with gold-conjugated binding domain of BoNT/A (22). Our collective data represent the first direct demonstration, by KD and/or KO, of the neuronal uptake and cytosolic translocation of BoNT by activity/clathrin/Amph/dynamin-dependent endocytosis. This process shares the initial path of vesicle recycling to acidic organelles, but the protease of toxin diverges from there by translocating into the cytosol to cleave its SNARE target, whereas the vesicular compartments continue in their own routes. Even though this process would exploit the direct retrieval of exocytosed vesicle proteins from the plasmalemma of CGNs, these might also be recovered indirectly *via* activity-dependent bulk endocytosis (ADBE), as inferred from the accumulation of membrane-associating dyes (60, 61). Although the earlier stages of ADBE do not require clathrin, and the initial endosomes involved do not acidify (60, 62), synaptic vesicles are eventually formed (and, presumably, do acidify) by budding later from the endosomes in a clathrin-dependent step (63). Thus, it is possible that some toxin may enter CGNs *via* ADBE, although the monitoring of SNAP-25 cleavage used in our study precluded this question being addressed directly. As ADBE has an absolute requirement for dynamin 1 (61, 64), it cannot be involved in toxin uptake into TGNs, because KO of this isoform failed to inhibit the entry of EA. Even in CGNs, ADBE could make only, at best, a minor contribution, because the KD of AP2α2 virtually abolished EA entry, whereas ADBE requires AP1 and AP3 but not AP2 (65–67). In this context, it is notable that the BoNT/A acceptor SV2 contains 2 AP2 binding motifs, whereas AP1 and AP3 have been reported to display less association with SV2A residues 1–163 (59).

Distinct isoforms of dynamin and Amph in neurons containing SCSVs or LDCVs mediate activity-dependent endocytosis and contribute to the different time-courses

Isoform-specific KO or KD revealed the preferential utilization of dynamins in activity-dependent BoNT entry, with a rank order of $1 \approx 2 > 3$ in CGNs compared with $3 > 2 \gg 1$ in TGNs. Ablation by either method of dynamin 1 reduced (~50%) evoked BoNT uptake into CGNs, with the remainder being afforded by dynamin 2 and 3, because inhibiting all the isoforms with dynasore blocked the evoked entry completely. This conclusion is supported by dynasore causing a more extensive delay in the quenching of SypHluorin than KO of dynamin 1. Indeed, KO of dynamin 1 merely slowed the decrease in fluorescence, in accord with isoform 1 being required for the initial fast phase of endocytosis in cortical neurons (42). In contrast, the retrieval of SypHluorin in TGNs was unaffected by the ablation of dynamin 1, consistent with the demonstrated lack of its recruitment to sites of synaptotagmin recycling visualized with Syt-ecto. Although the reasons for lack of recruitment of dynamin 1 to the plasma membrane in TGNs remain unresolved, speculative explanations include absence of its stimulated dephosphorylation (68) and/or alternative splicing in these cells (21). Presumably, the dynamin 1 in TGNs could be involved in other vesicle fission processes unrelated to endocytosis *e.g.*, formation of Golgi-derived vesicles, as suggested for dynamin 2 in non-neuronal cells (69). In view of this lack of involvement of dynamin 1, the significant delay in SypHluorin endocytosis caused by dynasore implicates dynamin 2 and 3; this deduction is strengthened by their observed colocalization with Syt-ecto. It is noteworthy that the func-

tional importance of dynamin 2 for the slower mode of evoked endocytosis in both CGNs and TGNs concurs with the slow residual compensatory endocytosis reported for cortical neurons from dynamin 1 and 3 double-KO mice (70). Interestingly, overexpression in cultured motor neurons of a dominant-negative mutant of dynamin 2 (K44A) blocked the endocytosis of a binding fragment from tetanus toxin, a protein closely related to BoNTs (71). Such utilization of distinct dynamins, as proposed for chromaffin cells (72), could arise from differential activation of the requisite isoforms by the dissimilar localized $[Ca^{2+}]_i$ required for the exocytosis of SCSVs and LDCVs (73). In this scenario, the Ca^2 requirements for activation of dynamins may underlie the observed absence of their involvement in the basal uptake of BoNT.

In terms of other proteins that mediate endocytosis *via* association with dynamins, it was intriguing to find the sole presence of Amph1 in TGNs, in contrast to both Amph1 and Amph2 in CGNs. In TGNs, KD of Amph1 demonstrated its requirement for evoked BoNT uptake, consistent with it residing close to dynamin 2 and being associated with isoforms 2 and 3 in an extract of these cells. A different situation was found for CGNs because KD of isoform 1 failed to alter the evoked uptake of BoNT, despite its proximity to dynamin 1 and 2 *in situ* and immunoisolation with all 3 dynamins. The most likely interpretation of these findings is that isoform 2 can compensate for the absence of isoform 1.

Finally, it is reasonable to deduce that the utilization of distinct isoforms of dynamin and Amph by central and sensory neurons facilitates the respective fast and slow retrieval of SCSV and LDCV constituents needed for their disparate biogenesis and trafficking. This, in turn, could contribute to the greater susceptibility to BoNTs of CGNs (or others) that release fast-acting neurotransmitters than TGNs (and various sensory neurons), which more slowly secrete modulatory peptides. FJ

This research is funded by a Principle Investigator Award (to J.O.D.) from Science Foundation Ireland, in part by Allergan Inc. (Irvine, CA, USA) and under the Neuroscience Section of the Programme for Research in Third Level Institutions (PRTLI) Cycle 4. The PRTLI is cofunded through the European Regional Development Fund (ERDF), part of the European Union Structural Funds Programme 2007–2013. The authors thank Pietro De Camilli (Yale University, New Haven, CT, USA) for providing dynamin 1 heterozygous mice and Dr. Shawn M. Ferguson (Yale University) for suggestions on breeding and genotyping. The authors are also grateful to Dr. Y. Zhu (Northwestern University, Evanston, IL, USA) for providing the SypHluorin construct.

REFERENCES

1. Montal, M. (2010) Botulinum neurotoxin: a marvel of protein design. *Annu. Rev. Biochem.* **79,** 591–617
2. Davletov, B., Bajohrs, M., and Binz, T. (2005) Beyond BOTOX: advantages and limitations of individual botulinum neurotoxins. *Trends Neurosci.* **28,** 446–452
3. Dolly, J. O., Wang, J., Zurawski, T. H., and Meng, J. (2011) Novel therapeutics based on recombinant botulinum neurotoxins to normalize the release of transmitters and pain mediators. *FEBS J.* **278,** 4454–4466
4. Dodick, D. W., Turkel, C. C., DeGryse, R. E., Aurora, S. K., Silberstein, S. D., Lipton, R. B., Diener, H. C., and Brin, M. F. (2010) OnabotulinumtoxinA for treatment of chronic migraine: pooled results from the double-blind, randomized, placebo-controlled phases of the PREEMPT clinical program. *Headache* **50,** 921–936
5. Jackson, J. L., Kuriyama, A., and Hayashino, Y. (2012) Botulinum toxin A for prophylactic treatment of migraine and tension headaches in adults: a meta-analysis. *JAMA* **307,** 1736–1745
6. Peng, L., Tepp, W. H., Johnson, E. A., and Dong, M. (2011) Botulinum neurotoxin D uses synaptic vesicle protein SV2 and gangliosides as receptors. *PLoS Pathog.* **7,** e1002008
7. Dong, M., Yeh, F., Tepp, W. H., Dean, C., Johnson, E. A., Janz, R., and Chapman, E. R. (2006) SV2 is the protein receptor for botulinum neurotoxin A. *Science* **312,** 592–596
8. Mahrhold, S., Rummel, A., Bigalke, H., Davletov, B., and Binz, T. (2006) The synaptic vesicle protein 2C mediates the uptake of botulinum neurotoxin A into phrenic nerves. *FEBS Lett.* **580,** 2011–2014
9. Dong, M., Liu, H., Tepp, W. H., Johnson, E. A., Janz, R., and Chapman, E. R. (2008) Glycosylated SV2A and SV2B mediate the entry of botulinum neurotoxin E into neurons. *Mol. Biol. Cell* **19,** 5226–5237
10. Fu, Z., Chen, C., Barbieri, J. T., Kim, J. J., and Baldwin, M. R. (2009) Glycosylated SV2 and gangliosides as dual receptors for botulinum neurotoxin serotype F. *Biochemistry* **48,** 5631–5641
11. Rummel, A., Hafner, K., Mahrhold, S., Darashchonak, N., Holt, M., Jahn, R., Beermann, S., Karnath, T., Bigalke, H., and Binz, T. (2009) Botulinum neurotoxins C, E and F bind gangliosides via a conserved binding site before stimulation-dependent uptake with botulinum neurotoxin F utilising the three isoforms of SV2 as second receptor. *J. Neurochem.* **110,** 1942–1954
12. Rummel, A., Karnath, T., Henke, T., Bigalke, H., and Binz, T. (2004) Synaptotagmins I and II act as nerve cell receptors for botulinum neurotoxin G. *J. Biol. Chem.* **279,** 30865–30870
13. Jin, R., Rummel, A., Binz, T., and Brunger, A. T. (2006) Botulinum neurotoxin B recognizes its protein receptor with high affinity and specificity. *Nature* **444,** 1092–1095
14. Dong, M., Tepp, W. H., Liu, H., Johnson, E. A., and Chapman, E. R. (2007) Mechanism of botulinum neurotoxin B and G entry into hippocampal neurons. *J. Cell Biol.* **179,** 1511–1522
15. Dong, M., Richards, D. A., Goodnough, M. C., Tepp, W. H., Johnson, E. A., and Chapman, E. R. (2003) Synaptotagmins I and II mediate entry of botulinum neurotoxin B into cells. *J. Cell Biol.* **162,** 1293–1303
16. Dolly, J. O., Black, J., Williams, R. S., and Melling, J. (1984) Acceptors for botulinum beurotoxin reside on motor-nerve terminals and mediate its internalization. *Nature* **307,** 457–460
17. Simpson, L. L. (1980) Kinetic studies on the interaction between botulinum toxin type A and the cholinergic neuromuscular junction. *J. Pharmacol. Exp. Ther.* **212,** 16–21
18. Black, J. D., and Dolly, J. O. (1986) Interaction of 125I-labeled botulinum neurotoxins with nerve terminals. II. Autoradiographic evidence for its uptake into motor nerves by acceptor-mediated endocytosis. *J. Cell Biol.* **103,** 535–544
19. Partoens, P., Slembrouck, D., Quatacker, J., Baudhuin, P., Courtoy, P. J., and De Potter, W. P. (1998) Retrieved constituents of large dense-cored vesicles and synaptic vesicles intermix in stimulation-induced early endosomes of noradrenergic neurons. *J. Cell Sci.* **111,** 681–689
20. Fischer, A., Nakai, Y., Eubanks, L. M., Clancy, C. M., Tepp, W. H., Pellett, S., Dickerson, T. J., Johnson, E. A., Janda, K. D., and Montal, M. (2009) Bimodal modulation of the botulinum neurotoxin protein-conducting channel. *Proc. Natl. Acad. Sci. U. S. A.* **106,** 1330–1335
21. Ferguson, S. M., and De Camilli, P. (2012) Dynamin, a membrane-remodelling GTPase. *Nat. Rev. Mol. Cell Biol.* **13,** 75–88
22. Harper, C. B., Martin, S., Nguyen, T. H., Daniels, S. J., Lavidis, N. A., Popoff, M. R., Hadzic, G., Mariana, A., Chau, N., McCluskey, A., Robinson, P. J., and Meunier, F. A. (2011)

Dynamin inhibition blocks botulinum neurotoxin type A endocytosis in neurons and delays botulism. *J. Biol. Chem.* **286,** 35966–35976
23. Haucke, V., and De Camilli, P. (1999) AP-2 recruitment to synaptotagmin stimulated by tyrosine-based endocytic motifs. *Science* **285,** 1268–1271
24. Collins, B. M., McCoy, A. J., Kent, H. M., Evans, P. R., and Owen, D. J. (2002) Molecular architecture and functional model of the endocytic AP2 complex. *Cell* **109,** 523–535
25. Zhang, J. Z., Davletov, B. A., Sudhof, T. C., and Anderson, R. G. (1994) Synaptotagmin I is a high affinity receptor for clathrin AP-2: implications for membrane recycling. *Cell* **78,** 751–760
26. Couesnon, A., Shimizu, T., and Popoff, M. R. (2009) Differential entry of botulinum neurotoxin A into neuronal and intestinal cells. *Cell. Microbiol.* **11,** 289–308
27. Lichte, B., Veh, R. W., Meyer, H. E., and Kilimann, M. W. (1992) Amphiphysin, a novel protein associated with synaptic vesicles. *EMBO J.* **11,** 2521–2530
28. Wigge, P., Kohler, K., Vallis, Y., Doyle, C. A., Owen, D., Hunt, S. P., and McMahon, H. T. (1997) Amphiphysin heterodimers: potential role in clathrin-mediated endocytosis. *Mol. Biol. Cell* **8,** 2003–2015
29. Wang, J., Meng, J., Lawrence, G. W., Zurawski, T. H., Sasse, A., Bodeker, M. O., Gilmore, M. A., Fernandez-Salas, E., Francis, J., Steward, L. E., Aoki, K. R., and Dolly, J. O. (2008) Novel chimeras of botulinum neurotoxins A and E unveil contributions from the binding, translocation, and protease domains to their functional characteristics. *J. Biol. Chem.* **283,** 16993–17002
30. Wang, J., Zurawski, T. H., Meng, J., Lawrence, G., Olango, W. M., Finn, D. P., Wheeler, L., and Dolly, J. O. (2011) A dileucine in the protease of botulinum toxin A underlies its long-lived neuroparalysis: transfer of longevity to a novel potential therapeutic. *J. Biol. Chem.* **286,** 6375–6385
31. Wang, J., Zurawski, T. H., Bodeker, M. O., Meng, J., Boddul, S., Aoki, K. R., and Dolly, J. O. (2012) Longer-acting and highly potent chimaeric inhibitors of excessive exocytosis created with domains from botulinum neurotoxin A and B. *Biochem. J.* **444,** 59–67
32. Meng, J., Wang, J., Lawrence, G., and Dolly, J. O. (2007) Synaptobrevin I mediates exocytosis of CGRP from sensory neurons and inhibition by botulinum toxins reflects their anti-nociceptive potential. *J. Cell Sci.* **120,** 2864–2874
33. Meng, J., Ovsepian, S. V., Wang, J., Pickering, M., Sasse, A., Aoki, K. R., Lawrence, G. W., and Dolly, J. O. (2009) Activation of TRPV1 mediates calcitonin gene-related peptide release, which excites trigeminal sensory neurons and is attenuated by a retargeted botulinum toxin with anti-nociceptive potential. *J. Neurosci.* **29,** 4981–4992
34. Macia, E., Ehrlich, M., Massol, R., Boucrot, E., Brunner, C., and Kirchhausen, T. (2006) Dynasore, a cell-permeable inhibitor of dynamin. *Dev. Cell* **10,** 839–850
35. Doherty, G. J., and McMahon, H. T. (2009) Mechanisms of endocytosis. *Annu. Rev. Biochem.* **78,** 857–902
36. Mayor, S., and Pagano, R. E. (2007) Pathways of clathrin-independent endocytosis. *Nat. Rev. Mol. Cell Biol.* **8,** 603–612
37. Von Kleist, L., Stahlschmidt, W., Bulut, H., Gromova, K., Puchkov, D., Robertson, M. J., MacGregor, K. A., Tomilin, N., Pechstein, A., Chau, N., Chircop, M., Sakoff, J., von Kries, J. P., Saenger, W., Krausslich, H. G., Shupliakov, O., Robinson, P. J., McCluskey, A., and Haucke, V. (2011) Role of the clathrin terminal domain in regulating coated pit dynamics revealed by small molecule inhibition. *Cell* **146,** 471–484
38. Urrutia, R., Henley, J. R., Cook, T., and McNiven, M. A. (1997) The dynamins: redundant or distinct functions for an expanding family of related GTPases? *Proc. Natl. Acad. Sci. U. S. A.* **94,** 377–384
39. Cao, H., Garcia, F., and McNiven, M. A. (1998) Differential distribution of dynamin isoforms in mammalian cells. *Mol. Biol. Cell.* **9,** 2595–2609
40. Yao, J., Kwon, S. E., Gaffaney, J. D., Dunning, F. M., and Chapman, E. R. (2011) Uncoupling the roles of synaptotagmin I during endo- and exocytosis of synaptic vesicles. *Nat. Neurosci.* **15,** 243–249
41. Lowe, A. W., Madeddu, L., and Kelly, R. B. (1988) Endocrine secretory granules and neuronal synaptic vesicles have three integral membrane proteins in common. *J. Cell Biol.* **106,** 51–59
42. Ferguson, S. M., Brasnjo, G., Hayashi, M., Wolfel, M., Collesi, C., Giovedi, S., Raimondi, A., Gong, L. W., Ariel, P., Paradise, S., O'Toole, E., Flavell, R., Cremona, O., Miesenbock, G., Ryan, T. A., and De Camilli, P. (2007) A selective activity-dependent requirement for dynamin 1 in synaptic vesicle endocytosis. *Science* **316,** 570–574
43. Matteoli, M., Takei, K., Perin, M. S., Sudhof, T. C., and De Camilli, P. (1992) Exo-endocytotic recycling of synaptic vesicles in developing processes of cultured hippocampal neurons. *J. Cell Biol.* **117,** 849–861
44. Zhu, Y., Xu, J., and Heinemann, S. F. (2009) Two pathways of synaptic vesicle retrieval revealed by single-vesicle imaging. *Neuron* **61,** 397–411
45. Bauerfeind, R., Takei, K., and De Camilli, P. (1997) Amphiphysin I is associated with coated endocytic intermediates and undergoes stimulation-dependent dephosphorylation in nerve terminals. *J. Biol. Chem.* **272,** 30984–30992
46. Liu, J. P., Sim, A. T., and Robinson, P. J. (1994) Calcineurin inhibition of dynamin I GTPase activity coupled to nerve terminal depolarization. *Science* **265,** 970–973
47. Soderberg, O., Gullberg, M., Jarvius, M., Ridderstrale, K., Leuchowius, K. J., Jarvius, J., Wester, K., Hydbring, P., Bahram, F., Larsson, L. G., and Landegren, U. (2006) Direct observation of individual endogenous protein complexes in situ by proximity ligation. *Nat. Methods* **3,** 995–1000
48. Feng, G., Mellor, R. H., Bernstein, M., Keller-Peck, C., Nguyen, Q. T., Wallace, M., Nerbonne, J. M., Lichtman, J. W., and Sanes, J. R. (2000) Imaging neuronal subsets in transgenic mice expressing multiple spectral variants of GFP. *Neuron* **28,** 41–51
49. Chai, Q., Arndt, J. W., Dong, M., Tepp, W. H., Johnson, E. A., Chapman, E. R., and Stevens, R. C. (2006) Structural basis of cell surface receptor recognition by botulinum neurotoxin B. *Nature* **444,** 1096–1100
50. Restani, L., Giribaldi, F., Manich, M., Bercsenyi, K., Menendez, G., Rossetto, O., Caleo, M., and Schiavo, G. (2012) Botulinum neurotoxins A and E undergo retrograde axonal transport in primary motor neurons. *PLoS Pathog.* **8,** e1003087
51. Black, J. D., and Dolly, J. O. (1986) Interaction of 125I-labeled botulinum neurotoxins with nerve terminals. I. Ultrastructural autoradiographic localization and quantitation of distinct membrane acceptors for types A and B on motor nerves. *J. Cell Biol.* **103,** 521–534
52. Yowler, B. C., Kensinger, R. D., and Schengrund, C. L. (2002) Botulinum neurotoxin A activity is dependent upon the presence of specific gangliosides in neuroblastoma cells expressing synaptotagmin I. *J. Biol. Chem.* **277,** 32815–32819
53. Kirkham, M., and Parton, R. G. (2005) Clathrin-independent endocytosis: new insights into caveolae and non-caveolar lipid raft carriers. *Biochim. Biophys. Acta* **1745,** 273–286
54. Chung, C., Barylko, B., Leitz, J., Liu, X., and Kavalali, E. T. (2010) Acute dynamin inhibition dissects synaptic vesicle recycling pathways that drive spontaneous and evoked neurotransmission. *J. Neurosci.* **30,** 1363–1376
55. Kirkham, M., Fujita, A., Chadda, R., Nixon, S. J., Kurzchalia, T. V., Sharma, D. K., Pagano, R. E., Hancock, J. F., Mayor, S., and Parton, R. G. (2005) Ultrastructural identification of uncoated caveolin-independent early endocytic vehicles. *J. Cell Biol.* **168,** 465–476
56. Hesse, S., Jahnke, M. T., Luecke, D., and Mauritz, K. H. (1995) Short-term electrical stimulation enhances the effectiveness of botulinum toxin in the treatment of lower limb spasticity in hemiparetic patients. *Neurosci. Lett.* **201,** 37–40
57. Yiangou, Y., Anand, U., Otto, W. R., Sinisi, M., Fox, M., Birch, R., Foster, K. A., Mukerji, G., Akbar, A., Agarwal, S. K., and Anand, P. (2011) Increased levels of SV2A botulinum neurotoxin receptor in clinical sensory disorders and functional effects of botulinum toxins A and E in cultured human sensory neurons. *J. Pain Res.* **4,** 347–355
58. Binz, T., and Rummel, A. (2009) Cell entry strategy of clostridial neurotoxins. *J. Neurochem.* **109,** 1584–1595
59. Yao, J., Nowack, A., Kensel-Hammes, P., Gardner, R. G., and Bajjalieh, S. M. (2010) Cotrafficking of SV2 and synaptotagmin at the synapse. *J. Neurosci.* **30,** 5569–5578
60. Kasprowicz, J., Kuenen, S., Miskiewicz, K., Habets, R. L., Smitz, L., and Verstreken, P. (2008) Inactivation of clathrin heavy chain inhibits synaptic recycling but allows bulk membrane uptake. *J. Cell Biol.* **182,** 1007–1016

61. Clayton, E. L., Anggono, V., Smillie, K. J., Chau, N., Robinson, P. J., and Cousin, M. A. (2009) The phospho-dependent dynamin-syndapin interaction triggers activity-dependent bulk endocytosis of synaptic vesicles. *J. Neurosci.* **29,** 7706–7717
62. Granseth, B., Odermatt, B., Royle, S. J., and Lagnado, L. (2006) Clathrin-mediated endocytosis is the dominant mechanism of vesicle retrieval at hippocampal synapses. *Neuron* **51,** 773–786
63. Clayton, E. L., and Cousin, M. A. (2009) The molecular physiology of activity-dependent bulk endocytosis of synaptic vesicles. *J. Neurochem.* **111,** 901–914
64. Clayton, E. L., Sue, N., Smillie, K. J., O'Leary, T., Bache, N., Cheung, G., Cole, A. R., Wyllie, D. J., Sutherland, C., Robinson, P. J., and Cousin, M. A. (2010) Dynamin I phosphorylation by GSK3 controls activity-dependent bulk endocytosis of synaptic vesicles. *Nat. Neurosci.* **13,** 845–851
65. Voglmaier, S. M., Kam, K., Yang, H., Fortin, D. L., Hua, Z., Nicoll, R. A., and Edwards, R. H. (2006) Distinct endocytic pathways control the rate and extent of synaptic vesicle protein recycling. *Neuron* **51,** 71–84
66. Newell-Litwa, K., Seong, E., Burmeister, M., and Faundez, V. (2007) Neuronal and non-neuronal functions of the AP-3 sorting machinery. *J. Cell Sci.* **120,** 531–541
67. Cheung, G., and Cousin, M. A. (2012) Adaptor protein complexes 1 and 3 are essential for generation of synaptic vesicles from activity-dependent bulk endosomes. *J. Neurosci.* **32,** 6014–6023
68. Tomizawa, K., Sunada, S., Lu, Y. F., Oda, Y., Kinuta, M., Ohshima, T., Saito, T., Wei, F. Y., Matsushita, M., Li, S. T., Tsutsui, K., Hisanaga, S., Mikoshiba, K., Takei, K., and Matsui, H. (2003) Cophosphorylation of amphiphysin I and dynamin I by Cdk5 regulates clathrin-mediated endocytosis of synaptic vesicles. *J. Cell Biol.* **163,** 813–824
69. Allan, V. J., Thompson, H. M., and McNiven, M. A. (2002) Motoring around the Golgi. *Nat. Cell Biol.* **4,** E236–242
70. Raimondi, A., Ferguson, S. M., Lou, X., Armbruster, M., Paradise, S., Giovedi, S., Messa, M., Kono, N., Takasaki, J., Cappello, V., O'Toole, E., Ryan, T. A., and De Camilli, P. (2011) Overlapping role of dynamin isoforms in synaptic vesicle endocytosis. *Neuron* **70,** 1100–1114
71. Deinhardt, K., Berninghausen, O., Willison, H. J., Hopkins, C. R., and Schiavo, G. (2006) Tetanus toxin is internalized by a sequential clathrin-dependent mechanism initiated within lipid microdomains and independent of epsin1. *J. Cell Biol.* **174,** 459–471
72. Artalejo, C. R., Elhamdani, A., and Palfrey, H. C. (2002) Sustained stimulation shifts the mechanism of endocytosis from dynamin-1-dependent rapid endocytosis to clathrin- and dynamin-2-mediated slow endocytosis in chromaffin cells. *Proc. Natl. Acad. Sci. U. S. A.* **99,** 6358–6363
73. Verhage, M., McMahon, H. T., Ghijsen, W. E., Boomsma, F., Scholten, G., Wiegant, V. M., and Nicholls, D. G. (1991) Differential release of amino acids, neuropeptides, and catecholamines from isolated nerve terminals. *Neuron* **6,** 517–524

Received for publication February 5, 2013.
Accepted for publication April 15, 2013.